

N O T I C E

THIS DOCUMENT HAS BEEN REPRODUCED FROM
MICROFICHE. ALTHOUGH IT IS RECOGNIZED THAT
CERTAIN PORTIONS ARE ILLEGIBLE, IT IS BEING RELEASED
IN THE INTEREST OF MAKING AVAILABLE AS MUCH
INFORMATION AS POSSIBLE

QUARTERLY REPORT

September 11, 1978 - December 10, 1978

CONTRACT NAS8-26749

TRENDS AND TECHNIQUES

FOR

SPACE BASE ELECTRONICS

Prepared for

**George C. Marshall Space Flight Center
Marshall Space Flight Center, Alabama 35812**

by

**J.D. Trotter
T.E. Wade
J.D. Gassaway**

**Microelectronics Research Laboratory
Mississippi State University
Department of Electrical Engineering
Mississippi State, Mississippi 39762**

1. REPORT NO.	2. GOVERNMENT ACCESSION NO.	3. RECIPIENT'S CATALOG NO.	
4. TITLE AND SUBTITLE A STUDY OF TRENDS AND TECHNIQUES FOR SPACE BASE ELECTRONICS		5. REPORT DATE January 1979	
		6. PERFORMING ORGANIZATION CODE MSU-EE-QUAR-79	
7. AUTHOR(S) J.D. Trotter, T.E. Wade, J.D. Gassaway		8. PERFORMING ORGANIZATION REPORT #	
9. PERFORMING ORGANIZATION NAME AND ADDRESS Department of Electrical Engineering Mississippi State University Mississippi State, MS 39762		10. WORK UNIT NO.	
		11. CONTRACT OR GRANT NO. NAS8-26749	
12. SPONSORING AGENCY NAME AND ADDRESS National Aeronautic and Space Administration Washington, D.C. 20546		13. TYPE OF REPORT & PERIOD COVERED Quarterly Progress September, 11, 1978-Dec. 10	
		14. SPONSORING AGENCY CODE	
15. SUPPLEMENTARY NOTES Prepared by Mississippi State University for George C. Marshall Space Flight Center, Marshall Space Flight Center, Alabama			
16. ABSTRACT In the third quarterly report, a brief progress report on the M.S.U. laboratory facilities will be presented in addition to the use of dry processing and alternate dielectrics. Emphasis will be placed on the two-dimensional MOSFET simulator. The two dimensional modeling program has been written for the simulation of short channel MOSFETs with nonuniform substrate doping. A key simplifying assumption used is that the majority carriers can be represented by a sheet charge at the silicon dioxide-silicon interface. In solving current continuity equation, the program does not converge. However, solving the 2-dimensional Poisson equation for the potential distribution has been achieved. The status of other 2-D MOSFET simulation programs are summarized.			
17. KEY WORDS MOSFETs 2-D modeling Modeling		18. DISTRIBUTION STATEMENT	
19. SECURITY CLASSIF. (of this report) Unclassified	20. SECURITY CLASSIF. (of this page) Unclassified	21. NO. OF PAGES	22. PRICE

TABLE OF CONTENTS

	Page
LIST OF ILLUSTRATIONS	11
I. MSU LABORATORY FACILITIES	1
II. DRY PROCESSING AND ALTERNATE DIELECTRICS	1
III. TWO-DIMENSIONAL MOSFET SIMULATION PROGRAM	4
IV. REFERENCES	30
V. QUARTERLY FINANCIAL STATEMENT	32

LIST OF ILLUSTRATIONS

Figure		Page
1.	MOSFET Cross-Section	9
2.	Grid system Definition	14
3.	Gauss's Law at The Silicon-Silicon Dioxide Interface	17
4.	Gauss's Law At The Source Corner	17

I. MSU LABORATORY FACILITIES

Negotiations are in progress with two semiconductor companies to donate surplus production equipment which include - (1) epi reactor and generator, (2) ion pump vacuum system, (3) vapox reactors, and (4) miscellaneous equipment for the hybrid laboratory.

II. DRY PROCESSING AND ALTERNATE DIELECTRICS

The exploratory processing involving dry chemistry required the use of plasma etching and plasma deposition equipment not available at either the Marshall Space Flight Center or Mississippi State University. Consequently, the logistics involved in processing the wafers have been difficult.

Four types of insulators were to be investigated:

- 1) 5% phosphorus doped silox,
- 2) plasma nitride,
- 3) the GAF version of polyimide, and
- 4) the Hitachi PIQ.

Whenever possible, dry chemistry processing was to be compared with "standard" wet chemistry. The wafers were processed through the first metal mask at Marshall Space Flight Center in standard fashion. The polyimide material was processed at American Microsystems, Inc. (AMI) using the standard recommend procedures by

the manufacturees. The nitride and silox were deposited at AMI using their standard processes, the former on an Applied Materials plasma reactor. The wet chemistry processing was performed at AMI using AMI's standard processing. The plasma etching was performed by Davis and Wilder on one of their production parallel plate plasma system using their proprietary processes.

The wet chemistry split involving silox was lost when the standard "pad" etch attacked the metal completely. The same batch etchant continued to provide good results on AMI material. Since the first layer metal at NASA was deposited via sputtering and with many different impurities, compared with approximately 1% Si:Al deposited with electron beam, the difference in the metal film is believed to be the source of the problem.

The plasma nitride material and silox material, deposited by AMI and plasma etched by Davis & Wilder, was processed without any problems other than long delays. This material plus the polyimide material has finally been received for the final processing here. Although, no electrical results are available at the present, the microscopic examination displays the expected sharper edges of the dry processed material vs. the standard wet chemistry.

In the meantime, the results of the in situ back sputtering experiment were obtained. As was expected, the in situ back sputtering split gave much improved yields over that for the standard material - the detail results being published elsewhere.

The results of these experiments points to the requirement to

very effectively remove the Al_2O_3 prior to the second metalization or minimize its formation during wafer processing to within the order of 30 Å which a good sintering treatment can reduce. The in situ cleaning forgives prior processing which tends to grow the Al_2O_3 such as photoresist removal and buffered HF etching of oxide.

The dry processing has the potential in the future of resolving smaller via sizes and, simultaneously, avoids the harmful H_2O to accelerate the aluminum oxide (and hydrate) formation. Although dry processing to remove the photoresist is routinely done one should expect Al_2O_3 formation due to the presence of active oxygen in the "ashing" process. Some parallel plate reactors can be modified to introduce Ar at low pressure and effectively as in a back sputtering mode. This latter mode could then be used as a clean up step prior to second metal deposition - although not in situ. Undoubtedly, dry processing is going to be extremely important in future double layer metal development work.

III. TWO-DIMENSIONAL MOSFET SIMULATION PROGRAM

A. Long Term Objective

The basic long term objective is to develop a two-dimensional computer program which derives the channel current in steady-state from given values of potential: source, drain, gate, and substrate. Also given are physical parameters such as gate length, dielectric thickness, doping levels, etc. The substrate doping level should be variable in two dimensions and the substrate potential is independent of the source potential in order to include body-bias effects. The program is intended to model MOSFETs with short channels with particular emphasis on subthreshold and punch-through conduction.

Secondary objective is to utilize techniques in the computer program to minimize computer run time while still maintaining reasonable simulation accuracy.

B. Introduction

At the beginning of this project no programs were available which satisfied the specified objectives. There has been considerable work in two-dimensional modelling of JFETs including the works of Kennedy and O'Brien [1] and Martin Reiser [2]. The

MESFET has also received attention in two-dimensional simulation, e.g., Barnes [3]. Various modes of MOSFET operation have been simulated or modeled using two-dimensional techniques, e.g. Schroeder and Muller [4] (saturation), Barron [5] (low level currents), Armstrong et al [6] (pinch-off), Kennedy [7] (effects of ionizing radiation), Kennedy and Marley [8] (saturation), Mock [9], Motta [10], El-Mansy and Boothroyd [11]. Although these works all contribute to the knowledge required in reaching the objective of this task, only the effort by Mock is sufficiently general to meet the objectives--and it is unavailable for public distribution.

The work by Barnes [3] described the application of the finite-element method to the analysis of the MESFET.

Further, the finite-element method has been used for some time in solving problems in mechanics and elasticity; however, it has only recently been applied to semiconductor problems. This method has the power to treat some problems, such as eigen-value problems, for which the finite-difference method is awkward if at all applicable. It can also be applied to the solution of field distributions governed by partial differential equations, and one of the most attractive features as compared to the finite-element method is purported to be the ease of treating non-rectangular geometries and irregular boundaries. For example, the geometry of the VMOS structure could be accommodated. It was decided to further investigate this technique.

The details of this evaluation are included in the appendix.

In summary, the evaluation resulted in some skepticism that the finite element method would be sufficiently effective for semiconductor problems to justify the effort. A more recent paper has reinforced this attitude. This paper indicates that the proper formulations of the semiconductor problem for the finite element approach remain to be demonstrated, and, in agreement with our observations, point out that the application of Galerkin's method is subject to skepticism. Therefore, it was concluded that the further work should be based upon the finite-difference method which we have used before although the finite-element method is intriguing and may be further developed in the future.

Key in the development of this task is the proper selection of assumptions. Certain assumptions are required to focus the effort and facilitate convergence expeditiously and, therefore, minimize computer time. On the other hand, too many assumptions lead to loss in utility.

The basic assumptions follow:

- 1) Recombination/generation is negligible.
- 2) Hole conduction is negligible.
- 3) The conventional expression for Poisson's equation is valid [see next section].
- 4) The mobile majority carriers are included in an infinitesimally thick layer of charge at the Si-SiO₂ interface.
- 5) The current flow in the channel is then described by a one-dimensional equation,

$$J_n = qD \frac{\partial S}{\partial x} + q \mu_n S E_x$$

where

- S = density of majority carriers in the channel,
- D = majority carrier diffusion constant,
- μ = channel carrier mobility, and
- E_x = tangential electric field component.

The first three sections are common in the stated literature and restrict the model from covering phenomena associated with breakdown and bulk generated leakage currents. The last assumption is key and separates this work seriously from that of Mock although Kennedy [7] used a similar approach for the sake of simplification.

Key also are the normal assumptions which are not made and which are commonly utilized:

- 1) the gradual channel approximation,
- 2) constant substrate doping, and
- 3) zero substrate bias.

Although a constant effective channel mobility is utilized during the initial development of the program, it is not intended to remain a basic assumption.

Assuming step junctions at the source (or drain), the potential in the depletion region and oxide is defined by Poisson's equation with appropriate boundary conditions (Figure 1):

- 1) fixed potential along the source (or drain) boundary (BCD and IJK),
- 2) fixed potential deep within the bulk substrate (AL),

3) zero horizontal component of electric field under the source and drain and far from the channel (AB and KL),

4) zero horizontal component of electric field in the oxide far from the channel (EF and KH) and

5) constant potential on the gate electrode (FG).

For convenience the substrate in the basic program is defined as having zero potential. The source, drain, and gate potentials are their respective applied potentials plus their work functions with respect to the substrate, i.e.,

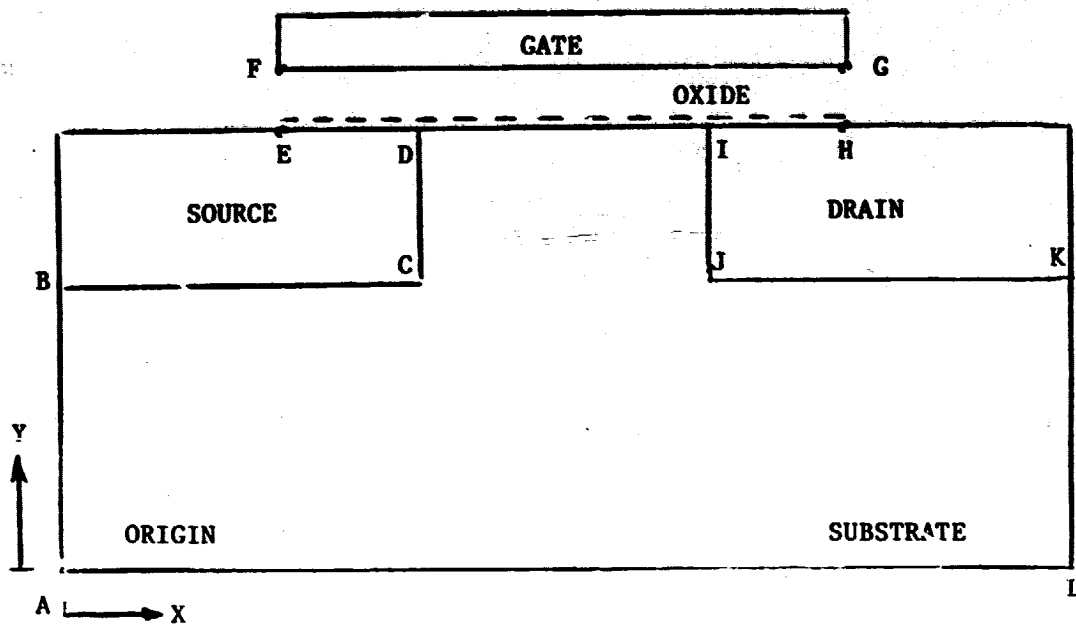
$$\psi_{\text{source}} = V_S + \phi_{\text{Bi}} \quad ,$$

$$\psi_{\text{drain}} = V_D + \phi_{\text{Bi}} \quad ,$$

$$\psi_{\text{gate}} = V_G + \phi_{\text{ms}} \quad .$$

For the NMOS example the potential ψ is always non-negative.

The gate dielectric is assumed to be ideal with infinite resistivity. The charge density in the dielectric is assumed to be zero except for a sheet charge representing the silicon-silicon dioxide interface charge Q_{ss} which is arbitrarily assumed to be $50 \text{ } \overset{\circ}{\text{A}}$ within the oxide at one grid spacing above the channel grid.



<u>DISTANCES</u>	<u>COORDINATES</u>
$AB = YDIST - YDIF$	$A = (1, 1)$
$CD = JI - YDIF$	$B = (1, JK1)$
$EF = HG = TOX$	$C = (IK, JKI)$
$BC = JK = XDIF$	$D = (IK, JMAX)$
$AL = XDIST$	$F = (IK5, JL)$
	$G = (IL5, JL)$
	$I = (IL, JMAX)$
	$K = (IMAX, JK1)$
	$L = (IMAX, 1)$
<u>OTHER RELATIONSHIPS</u>	
$IK5 = IK - 5, IL5 = IL + 5$	
$JL\phi = JL - 1, JK = JK1 - 1$	
$JMAX1 = JMAX + 1$	
$JMAX\phi = JMAX - 1$	

Figure 1. MOSFET Cross-Section

Key to the simulation of short channel devices is solving the two-dimensional Poisson's equation without making unnecessary approximations. The finite-difference formulation for Poisson's equation is given in the next section. The majority carrier charge is neglected in this formulation except for the sheet charge representation at the oxide interface. The intent is to ignore the charge where it is negligible compared with the ionized doping charge--which is a good assumption everywhere except in the channel.

One can then solve Poisson's equation for the two-dimensional potential distribution more easily and faster than if the coupled majority carrier current equation is included and the majority carrier density variable is included for every mesh node.

After finding the potential distribution one can, after the fact, explicitly solve for the majority carrier densities and current in order to predict punch-thru and subthreshold conduction behavior. This approach is aimed at minimizing computation time while retaining the essential relationships to maintain sufficient accuracy for modeling purposes. One should expect a compromise in accuracy, under certain conditions, when compared with the more general approach of solving the two-dimensional conduction equation.

C. The Poisson Equation, Difference Form

The Poisson equation in different form is

$$\nabla^2 \psi = - \rho / \epsilon \quad (1)$$

where

ψ = electrostatic potential,

ρ = charge density, and

ϵ = permittivity of the material.

For acceptor doped material the charge density is

$$\rho = q(p - nN_a) \quad , \quad \text{depletion,} \quad (2)$$

where

q = charge density,

p = hole density,

n = electron density, and

N_a = ionized acceptor density.

The hole density is defined by

$$p = N_a \exp(-u) \quad (3)$$

where

$u = q\psi/kT$, the normalized
potential, and

$u = 0$ in the charge neutral bulk.

Consequently, in the bulk substrate and in the depletion layer where the electron density can be neglected,

$$\rho = -q N_a [1 - \exp(-u)] \quad . \quad (4)$$

In the channel region the assumption is made that the electrons exists only in a sheet form of infinitesimal thickness at the silicon dioxide-silicon interface. Since the hole density is insignificant at inversion, the charge density in the channel is

$$\rho_s = -q(N_a S + n_s) \quad , \quad \text{channel,} \quad (5)$$

where

N_{aS} is the effective sheet charge due to the ionized acceptors within the grid spacing defined by the interface grid, and n_S is the sheet charge of electrons in the channel.

Near the oxide-silicon interface there are positive interface charges of density N_{SS} , consequently,

$$\rho = qN_{SS} \text{ , interface.} \quad (6)$$

with the location being assumed to be 50 \AA inside of the oxide. Otherwise in the oxide the charge is assumed neutral.

$$\rho = 0 \text{ , oxide,} \quad (7)$$

To solve the Poisson equation numerically, the left hand side can be expanded in difference form as

$$\begin{aligned} \nabla^2 \psi &= V_T \nabla^2 U \\ &= V_T [A U_{i,j-1} + B U_{i-1,j} + C U_{i,j} \\ &\quad + D U_{i+1,j} + E U_{i,j+1}] \end{aligned} \quad (8)$$

where $V_T = kT/q$,

$$A = 2[h_{j-1}(h_{j-1} + h_j)]^{-1},$$

$$B = 2[w_{i-1}(w_{i-1} + w_i)]^{-1},$$

$$D = 2[w_i(w_{i-1} + w_i)]^{-1},$$

$$E = 2[h_j(h_{j-1} + h_j)]^{-1}, \text{ and}$$

$$C = -(A + B + D + E)$$

with the grid system defined in Figure 2.

Using the charge equation (14) the complete Poisson equation in finite-difference form is written for node (i,j) as

$$\begin{aligned} A(i,j)U_{i,j-1} + B(i,j)U_{i-1,j} + C(i,j)U_{i,j} + D(i,j)U_{i+1,j} \\ + E(i,j)U_{i,j+1} = \frac{qN_a}{\epsilon V_T} [1 - \exp(-U_{i,j})] \end{aligned} \quad (9)$$

The above nonlinear equation can be linearized by defining a function F such that

$$\begin{aligned} F(U_{i,j-1}, U_{i-1,j}, U_{i,j}, U_{i+1,j}, U_{i,j+1}) &= F_{i,j} \\ &= A(i,j)U_{i,j-1} + B(i,j)U_{i-1,j} + C(i,j)U_{i,j} \\ &\quad + D(i,j)U_{i+1,j} + E(i,j)U_{i,j+1} \\ &\quad - (qN_a/\epsilon V_T) [1 - \exp(-U_{i,j})] = 0 \end{aligned} \quad (10)$$

Defining a set of reference value of U's and F such that

$U_{i,j-1}^r, U_{i-1,j}^r, U_{i,j}^r$, etc. and $F_{i,j}^r$, one can expand F around the

reference potentials:

$$\begin{aligned} F_{i,j}^{r+1} &= F_{i,j}^r + \left. \frac{\partial F}{\partial U_{i,j-1}} \right|_r \Delta U_{i,j-1} + \left. \frac{\partial F}{\partial U_{i-1,j}} \right|_r \Delta U_{i-1,j} \\ &\quad + \left. \frac{\partial F}{\partial U_{i,j}} \right|_r \Delta U_{i,j} + \left. \frac{\partial F}{\partial U_{i+1,j}} \right|_r \Delta U_{i+1,j} + \left. \frac{\partial F}{\partial U_{i,j+1}} \right|_r \Delta U_{i,j+1} \end{aligned} \quad (11)$$

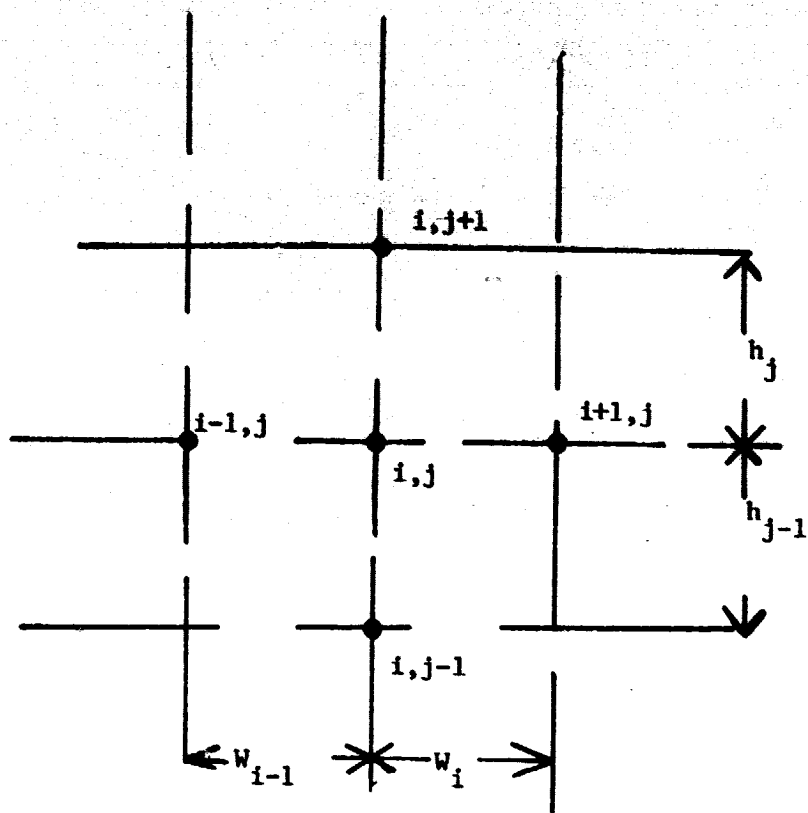


Figure 2. Grid system definition

where

$$\Delta U_{i,j-1}^r = U_{i,j-1}^{r+1} - U_{i,j-1}^r, \text{ etc.}$$

The above expressions defines a system of equations in ΔU as

$$\begin{aligned} F_{i,j}^r = & \bar{A}(i,j) \Delta U_{i,j-1} + \bar{B}(i,j) \Delta U_{i-1,j} + \bar{C}(i,j) \Delta U_{i,j} \\ & + \bar{D}(i,j) \Delta U_{i+1,j} + \bar{E}(i,j) \Delta U_{i,j+1} + F_{i,j}^r \end{aligned} \quad (12)$$

where

$$\bar{A} = A, \bar{B} = B, \bar{D} = D, \bar{E} = E, \text{ and}$$

$$\bar{C} = C - (qNa/kT) \exp(-U_{i,j}^r)$$

with A through E being defined in equation (8). The function F is theoretically zero; therefore, by setting $F_{i,j}^{r+1} = 0$, a system of linear equations in ΔU is obtained. For the node i,j

$$\begin{aligned} \bar{A} \Delta U_{i,j-1} + \bar{B} \Delta U_{i-1,j} + \bar{C} \Delta U_{i,j} \\ + \bar{D} \Delta U_{i+1,j} + \bar{E} \Delta U_{i,j+1} = - F_{i,j}^r \end{aligned} \quad (13)$$

where $F_{i,j}^r$ is defined in equation (10).

By applying the method of lines, the linearized equations are resolved into a tridiagonal matrix form as

$$\begin{aligned} \bar{A} \Delta U_{i,j-1} + \bar{C} \Delta U_{i,j} + \bar{E} \Delta U_{i,j+1} \\ = - F_{i,j}^r - \bar{B} \tilde{U}_{i-1,j} - \bar{D} \tilde{U}_{i+1,j} \end{aligned} \quad (14)$$

where \tilde{U} are taken as the most recent updated values of ΔU each iteration, but still keeping the U's fixed until convergence

is achieved. The above equation (14) retains the old values of ΔU along the x-axis and calculates the new values of ΔU along the y-axis. Obviously, equation (14) can be written for the inverse case. By alternating between the vertical and horizontal forms of the tridiagonal matrix, the convergence can be expedited.

Special consideration must be given to Poisson's equation at the silicon-silicon dioxide interface. Figure (3) illustrates the channel sheet charge S in charge per unit area, the acceptor charge N_a in charge per unit volume, and the discontinuity in permittivity. Applying Gauss's law in one dimension with two surfaces at the midway points between C & $C + 1$ and $C - 1$ & C leads to the expression

$$\begin{aligned} \epsilon_{ox} E_{1/2} - \epsilon_{Si} E_{-1/2} &= \text{positive charge enclosed} & (15) \\ &= -q \left(S + \frac{N_a h_{c-1}}{2} \right) \end{aligned}$$

Multiplying through by $\frac{2}{V_T (h_c + h_{c-1}) \epsilon_{Si}}$ leads to

$$\frac{2}{h_c + h_{c-1}} \left[\frac{\epsilon_{ox}}{\epsilon_{Si}} \left(\frac{U_{c+1} - U_c}{h_c} + \frac{U_{c-1} - U_c}{h_{c-1}} \right) \right] = \frac{Zq}{\epsilon_{Si} V_T} \frac{S + \frac{N_a h_{c-1}}{2}}{h_c + h_{c-1}} \quad (16)$$

which is the one dimension form of Poisson's Law

$$\frac{d^2}{dy^2} \left(\frac{\epsilon U}{\epsilon_{Si}} \right) = - \frac{\epsilon_{eff}}{\epsilon_{Si}} \quad (17)$$

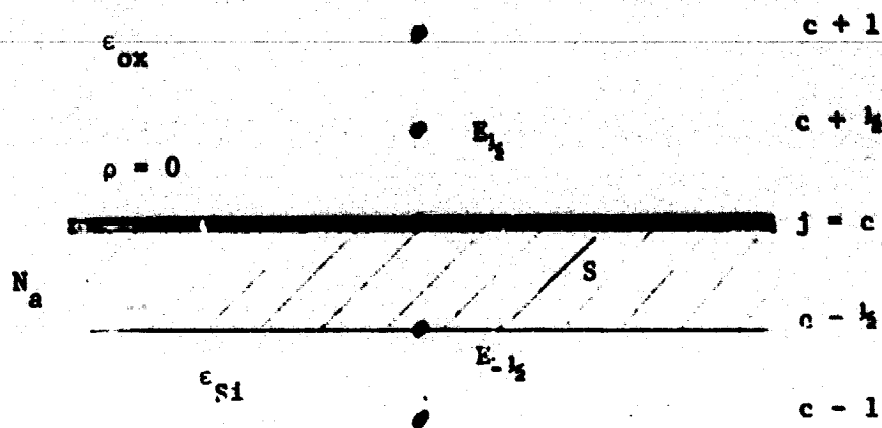


Figure 3. Gauss's law at the silicon-silicon dioxide interface

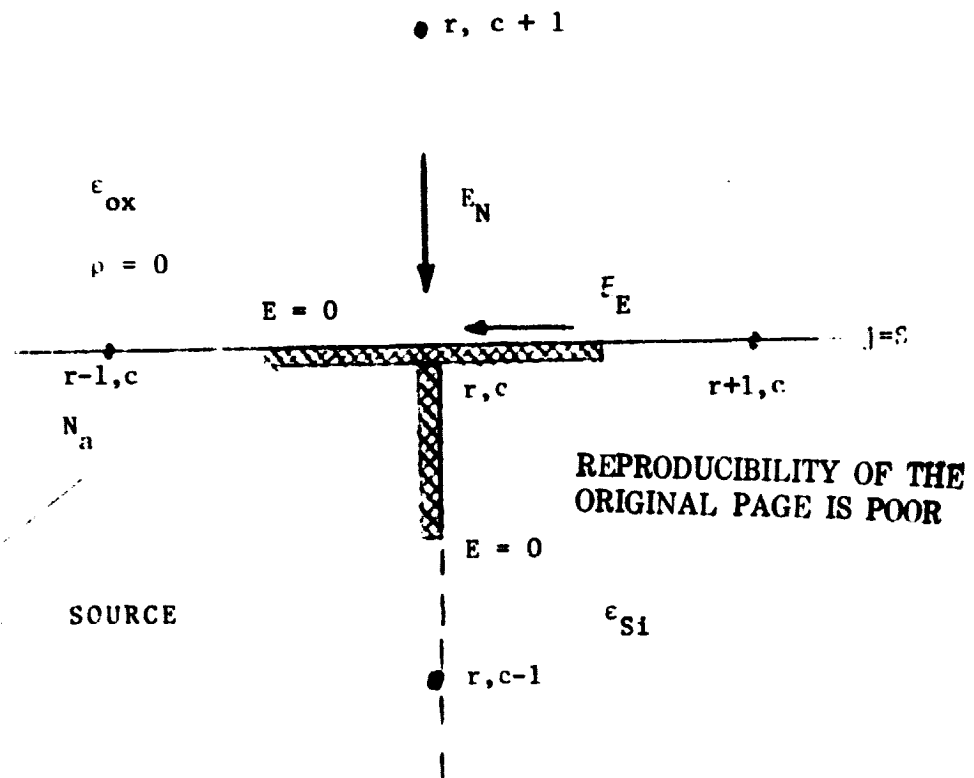


Figure 4. Gauss's law at the source corner

with

$$\rho_{\text{eff}} = - \frac{2q(S + N_a h_{c-1}/2)}{V_T (h_c + h_{c-1})}$$

Therefore, the finite difference form of the equation is obtained by modifying the following terms in equation (9):

$$E = 2 \left(\frac{\epsilon_{\text{ox}}}{\epsilon_{\text{Si}}} \right) [h_c (h_{c-1} + h_c)]^{-1}, \quad (18)$$

$$C = -(A + B + D + E), \quad \text{and}$$

$$\frac{\rho_{\text{eff}}}{\epsilon_{\text{Si}}} = \frac{2q}{V_T \epsilon_{\text{Si}}} \frac{(S + N_a h_{c-1}/2)}{(h_c + h_{c-1})}$$

[Note: $y = J_{\text{max}}$ for the channel node in the program.]

Similarly the linearized version is modified by

$$\bar{E}_i = E_i, \quad \bar{C}_i = C_i, \quad \text{and} \quad (19)$$

$$F_{i,c}^r = A_i U_{i,c-1} + B_i U_{i-1,c} + C_i U_{i,c} \\ + D_i U_{i+1,c} + E_i U_{i,c+1} + \rho_{\text{eff}}^i / \epsilon_{\text{Si}}$$

where the subscript i has been inserted to denote the coefficients for mesh node (i,c) .

In the region of $\text{Si} - \text{SiO}_2$ interface where the Q_{SS} charges are assumed to exist, one mesh node is assumed inside the oxide, the coefficients are

$$\bar{A} = A, \quad \bar{B} = B, \quad \bar{C} = C, \quad \bar{D} = D, \quad \bar{E} = E, \quad \text{and}$$

$$F^r = Au_{i,c} + BU_{i-1,c+1} + CU_{i,c+1} + DU_{i+1,c+1} + EU_{i,c+2} + \frac{2Q_{SS}}{\epsilon_{ox} V_T} [h_c + h_{c+1}]^{-1} \quad (20)$$

Similarly, in the oxide where $\rho = 0$, the coefficients are

$$\bar{A} = A, \bar{B} = B, \bar{C} = C, \bar{D} = D, \bar{E} = E, \text{ and} \quad (21)$$

$$F^r = AU_{i,j-1} + BU_{i-1,j} + CU_{i,j} + DU_{i+1,j} + EU_{i,j+1}$$

D. The Channel Conduction Equation, Difference Form

As noted previously, a significant assumption utilized to facilitate convergence, is that the channel charge is modeled as a sheet charge at the silicon-silicon dioxide interface. The channel current is assumed to obey the single dimensional form of the conventional three dimensional equation, i.e.,

$$J_n = q D_n \frac{\partial S}{\partial x} + q \mu_n S E_x \quad (22)$$

where S = density of electrons in channel (#per unit area),
 D_n = electron diffusion constant,
 μ_n = electron mobility, normally field dependent, and
 E_x = tangential electric field component.

The above equation can be written in normalized form utilizing

$$E_x = V_T \frac{\partial U}{\partial x} \text{ and } D_n = V_T \mu_n \text{ (Einstein's relationship):}$$

$$J_n = q V_T \mu_n \left(\frac{\partial S}{\partial x} - S \frac{\partial U}{\partial x} \right) \quad (23)$$

Then $f_s = (S - US) \mu_n$ (24)

where $f_s = J_n (q V_T)^{-1}$, $S' = \frac{\partial S}{\partial x}$, and $U' = \frac{\partial U}{\partial x}$.

At any point x in the channel the general solution of S is

$$S(x) = \exp \int_{x_{i-1}}^x U' dx \left\{ \int_{x_{i-1}}^x \left(\frac{f_s}{\mu_n} \exp \int_{x_{i-1}}^x U' dx \right) dx + C \right\} \quad (25)$$

which reduces to the specific solution for $S(x)$, given

S at $x = x_{i-1}$:

$$S(x) e^{-U} = S_{i-1} e^{-U_{i-1}} + \frac{J_n}{q V_T} \int_{x_{i-1}}^x \frac{e^{-u(\xi)}}{\mu(\xi)} d\xi \quad (26)$$

Rewriting the above leads to S_i in terms of S_{i-1} :

$$\frac{S_i \exp(-U_i) - S_{i-1} \exp(-U_{i-1})}{\int_{x_{i-1}}^{x_i} \frac{\exp(-U(\xi)) d\xi}{\mu(\xi)}} = \frac{J_n}{q V_T} \quad (27)$$

Similarly, integrating between x_i and x_{i+1} leads to

$$\frac{S_{i+1} \exp(-U_{i+1}) - S_i \exp(-U_i)}{\int_{x_i}^{x_{i+1}} \frac{\exp(-U(\xi)) d\xi}{\mu(\xi)}} = \frac{J_n}{q V_T} \quad (28)$$

Assuming current continuity, i.e., $J_n = \text{constant}$, leads to

$$\begin{aligned}
& - \left\{ \exp - (U_{i-1}) \int_{x_i}^{x_{i+1}} \frac{\exp - U(\xi) d \xi}{\mu(\xi)} \right\} S_{i-1} & (29) \\
& + \left\{ \exp - U_i \int_{x_{i-1}}^{x_{i+1}} \frac{\exp (U(\xi)) d \xi}{\mu(\xi)} \right\} S_i \\
& - \left\{ \exp - U_{i+1} \int_{x_{i-1}}^{x_i} \frac{\exp (-U(\xi)) d \xi}{\mu(\xi)} \right\} S_{i+1} = 0 .
\end{aligned}$$

The above equation is of the form

$$a_i S_{i-1} + b_i S_i + c_i S_{i+1} = 0$$

and define a tridiagonal linear system of equations.

Equation 27 should reduce to a familiar form as $x_i - x_{i-1} = \Delta x \rightarrow 0$.

Let $S_{i-1} = S_o$, $S_i = S_o + \Delta S$, $U_{i-1} = U_o$, $U_i = U_o + \Delta U$. Then 27 becomes

$$\frac{(S_o + \Delta S) e^{-U_o} (1 - \Delta U) - S_o e^{-U_o}}{\mu^{-1} e^{-U_o} \Delta x} = \frac{J_n}{qV_T} \quad (30)$$

which reduces to

$$J_n = qV_T \mu \left\{ \frac{\Delta S}{\Delta x} - S_o \frac{\Delta U}{\Delta x} \right\} \quad (31)$$

which displays the familiar diffusion and drift terms in the limit.

The integral form in (27) has the potential of being more accurate with larger grid spacing.

Another observation one may note is that the coefficients

a_i , b_i , c_i may be scaled, or normalized, to values less dependent

on the exponential of potential by multiplying them by $\exp(2U_i)$

which gives

$$a_i = - \exp(U_i - U_{i-1}) \int_{x_i}^{x_{i+1}} \mu(\xi) \exp[U_i - U(\xi)] d\xi,$$

$$b_i = \int_{x_{i-1}}^{x_{i+1}} \mu^{-1}(\xi) \exp[U_i - U(\xi)] d\xi, \quad \text{and}$$

$$c_i = \exp(U_i - U_{i+1}) \int_{x_{i-1}}^{x_i} \mu^{-1}(\xi) \exp[U_i - U(\xi)] d\xi. \quad (32)$$

And, of course, if the mobility is assumed constant, then it can be removed by multiplying through by μ .

Noting that the integrand varies exponentially with potential whereas the potential is expected to vary with x no worse than the third power, one can approximate the integral by assuming

$$U - U_0 = a(x - x_0) \quad (33)$$

and evaluate the slope $a = \frac{dU}{dx}$ at the lowest value of potential over the range of integration. In this manner the neglected higher order terms contribute very little error since the integrand falls off exponentially with potential. Changing variables for the integration of b_i , as an example, leads to

$$b_i = \int_{U_{i-1}}^{U_{i+1}} \frac{\mu^{-1}(U)}{a} \exp[U_i - U] dU \quad (34)$$

where

$$a = \frac{dU}{dx}. \quad \text{Further,}$$

$$b_i = [a\mu]^{-1} (\exp(U_i - U_{i-1}) - \exp(U_i - U_{i+1})) \quad (35)$$

with a and μ evaluated at the lowest value of U which for $a > 0$ is U_{i-1} . Similarly,

$$\begin{aligned} a_i &= [a\mu]_i^{-1} [\exp(U_i - U_{i+1}) - 1] \exp(U_i - U_{i-1}) \\ c_i &= [a\mu]_{i-1}^{-1} [1 - \exp(U_i - U_{i-1})] \exp(U_i - U_{i+1}) \\ b_i &= [a\mu]_{i-1}^{-1} [\exp(U_i - U_{i-1}) - \exp(U_i - U_{i+1})] \end{aligned} \quad (36)$$

where the subscript on $[a\mu]$ denotes the node for evaluating a and μ , assuming $a > 0$.

The boundary conditions for this system of equations association with electron conduction in the channel must be defined in terms of the source and drain corner mesh nodes for the MOSFET operation in the active region. Figure 4 illustrates the application of Gauss's Law at the source corner of the channel. Mesh nodes along the boundary of the source are common potential, therefore, the tangential electric field terms along the boundary of the source are zero. Since the electric field along the channel E_E for operations of interest - at least at this source corner, the surface charge is modelled in a single dimensional manner, i.e.,

$$\epsilon_{ox} E_N = -qS \quad (37)$$

or, in terms of potential,

$$\frac{V_T \epsilon_{ox} (U_{r,c+1} - U_{r,c})}{h_c} = qS \quad (38)$$

An alternate scheme involves the solution of the one dimensional Poisson equation:

$$-\frac{\epsilon_{ox}}{t_{ox}} \left\{ (V_G - \phi_{ms}) - (V_C + V_{Bi}) \right\} = Q_{ss} - qS + Q_B \quad (39)$$

where V_G = the applied bias to the gate

ϕ_{ms} = the gate work function relative to the substrate,

V_C = the applied channel potential,

V_{Bi} = the work function of the drain/source,

t_{ox} = oxide thickness,

ϵ_{ox} = oxide permittivity,

Q_{ss} = silicon dioxide-silicon interface charge,

q = electronic charge, and

Q_B = the bulk charge density (per unit area)

= 0 for drain and source.

The Q_B expression can be defined in terms of the vertical electric field in the channel region:

$$Q_B = \epsilon V_T \frac{(U_{c-1} - U_c)}{h_{c-1}} - q N_a \frac{h_{c-1}}{2}$$

where the subscript c refers to the channel node.

E. Channel Coupled Equations

Although the channel conduction equation (29) is linear in S , it is nonlinear in potential. The simultaneous solution of the conduction equation and the Poisson equation along the channel

requires linearizing (29).

Let $F_{ci}^r = a_i S_{i-1} + b_i S_i + c_i S_{i+1}$ where a_i, b_i, c_i are defined in (36). Since the terms $[\alpha\mu]^{-1}$ vary more slowly than the exponential terms, the term is assumed constant for any particular iteration, using the last known values of u 's for its evaluation. Then, the linearized conduction equation becomes

$$A_{ci} = \frac{\partial F_{ci}^r}{\partial U_{i-1}} = -a_i S_{i-1} [\alpha\mu]_{i-1}^{-1} S_i \exp(U_i - U_{i-1}) + c_i S_{i+1} \exp(U_i - U_{i-1}) [1 - \exp(U_i - U_{i-1})]^{-1},$$

$$B_{ci} = a_i.$$

$$C_{ci} = \frac{\partial F_{ci}^r}{\partial U_i} = -a_i S_{i-1} [\exp(U_i - U_{i+1}) - 1]^{-1} + b_i S_i + c_i S_{i+1} [1 - \exp(U_i - U_{i-1})]^{-1} [1 - 2 \exp(U_i - U_{i-1})],$$

$$D_{ci} = b_i,$$

$$E_{ci} = \frac{\partial F_{ci}^r}{\partial U_{i+1}} = -a_i S_{i-1} \exp(U_i - U_{i+1}) [\exp(U_i - U_{i-1}) - 1]^{-1} + b_i S_i \exp(U_i - U_{i+1}) [\exp(U_i - U_{i-1}) - \exp(U_i - U_{i+1})]^{-1} - c_i S_{i+1},$$

$$G_{ci} = c_i, \text{ and}$$

$$F_{ci}^{r+1} = F_{ci}^r + A_{ci} \Delta U_{i-1} + B_{ci} \Delta S_{i-1} + C_{ci} \Delta U_i + D_{ci} \Delta S_i \quad (40)$$

$$+ E_{ci} \Delta U_{i+1} + G_{ci} \Delta U_{i+1} = 0.$$

The Poisson equation has been previously derived, equations (18) and (19), with the coefficients being defined below for the new system of equations:

$$\bar{B}_i \Delta U_{i-1,c} + \bar{C}_i \Delta U_{ic} + \bar{H}_i \Delta S_i + D_i \Delta U_{i+1,c} = -\bar{A}_i \Delta U_{i,c-1} - \bar{E}_i \Delta U_{i,c+1} - F_{i,c}^r = T_{ic}^r \quad (41)$$

where

$$\bar{H}_i = -2q[\epsilon_{si} V_T (h_{i,c} + h_{i,c-1})]^{-1},$$

$$\bar{A}_i = A_i \text{ from (17) ,}$$

$$\bar{B}_i = B_i \text{ from (17) ,}$$

$$\bar{D}_i = D_i \text{ from (17) ,}$$

$$\bar{E}_i = E_i \text{ from (17) ,}$$

$$C_i = C_i \text{ from (17) ,}$$

$$\bar{F}_{i,c}^r = \text{as defined in (28) .}$$

Simultaneously solving for the channel potential and the change charge requires the simultaneous solution of the above two equations (40) and (41) which results in the following system of equation in matrix form:

$$\begin{bmatrix} \bar{C} & \bar{H} & \bar{D} & 0 & 0 & 0 & \cdot & \cdot & \cdot & \cdot & \cdot \\ C & D & E & G & 0 & 0 & \cdot & \cdot & \cdot & \cdot & \cdot \\ \bar{B} & 0 & \bar{C} & \bar{H} & \bar{D} & 0 & \cdot & \cdot & \cdot & \cdot & \cdot \\ A & B & C & D & E & G & 0 & \cdot & \cdot & \cdot & \cdot \\ 0 & 0 & \bar{B} & 0 & \bar{C} & \bar{H} & \bar{D} & 0 & \cdot & \cdot & \cdot \\ 0 & 0 & A & B & C & D & E & G & 0 & \cdot & \cdot \\ & & / & / & / & / & / & / & & & \end{bmatrix} \begin{bmatrix} \Delta U_2 \\ \Delta S_2 \\ \Delta U_3 \\ \Delta S_3 \\ \cdot \\ \cdot \\ \cdot \\ \Delta U_{N-1} \\ \Delta S_{N-1} \end{bmatrix} = \begin{bmatrix} T_{2c} \\ -F_{2c} \\ T_{3c} \\ -F_{3c} \\ \cdot \\ \cdot \\ \cdot \\ T_{N-1,c} \\ -F_{N-1,c} \end{bmatrix}$$

The matrix is a 6 diagonal matrix. The number of variables is twice the number of grid points within the channel--not counting the boundary nodes at the source or drain. The solution can be conveniently solved by using a Gaussian elimination technique.

F. Overall Flow Chart

In order to expedite convergence, initially, the gradual channel approximation is assumed and the potential is calculated along the channel. This analytical approach divides the device cross-section into two regions, the channel, silicon substrate region and the oxide region.

In each of the two regions an initial approximation of the potential distribution is obtained by solving the one-dimensional form of Poisson's equation utilizing the given boundary potentials including the channel potential derived in the previous step. The one-dimensional equation is equivalent to setting $dU/dx = 0$. The potential distribution is found along one column (vertical) simultaneously. By sweeping in the x direction, i.e., repeat the solution on another column, the potential distribution for the entire region(s) is obtained.

Next the solution to the two dimensional P. E. is obtained in each region. In the oxide the potential along a column is obtained with the region being swept in the x-direction. In the silicon convergence is expedited by using the alternating direction implicit (ADI) scheme. First, the potential in the row below the channel (JMAX0) is obtained. Next the potential distributions for

each row between the source and drain are obtained by sweeping in the negative y-direction. When the solution to row JKL is obtained, the solution to the column $I = 1$ is obtained. The column solutions are obtained by sweeping in the positive x-direction. This ADI scheme is repeated until satisfactory convergence is obtained.

With the two-dimensional potential distribution obtained for both regions based on the gradual channel assumption, a new estimate of the channel potential and the channel charge is obtained by solving simultaneously the P. E. and current equation along the channel row. The 2-D P. E. is then solved along the rows between the source and drain by sweeping y in the negative direction. Next the columns solutions are obtained sweeping the x-direction for the entire regions--thus crossing the channel in the appropriate locations ($I = IK + 1$ to $IL-1$). This ADI scheme starting at the simultaneous solution of the P. E. and the current equation along the channel row is repeated until satisfactory convergence is obtained.

The channel current is obtained from an explicit solution to the channel current equation after the channel charge and potential are found.

G. Availability of 2-D MOSFET Simulators

The first 2-D simulator program which could provide I-V characteristics was developed by Mock [9] and Kennedy [8] at IBM in the 1970 to 1972 timeframe. The program, based on finite difference techniques, is proprietary to IBM. However, a modified

substrate bias.

Kennedy at the Applied Electronics Research Corporation has modified the Sutherland program to include provisions for

- 1) 1-D substrate impurity profile,
- 2) mobility dependence on gate voltage, and
- 3) substrate bias

and is now licensing the program (NEMOS) for \$10,000 for one year and \$7,500 for each succeeding year.

In addition, Hitachi has developed a finite element version with provisions, at least, for substrates with 1-D impurity profiles. Dr. Asai of Hitachi has indicated the possibility of licensing the program to Universities, government and industry in the United States. The Hitachi program called CADDET was developed in 1977-1978.

At least one other 2-D simulation program is under development. Jim Meindl at Stanford is under contract with ARPA to continue the work by Sutherland.

At this writing the author has been unable to determine when the program under development at Stanford will be available for distribution.

REFERENCES

1. Kennedy, D. P. and R. R. O'Brien, "Computer Aided Two-Dimensional Analysis of the Junction Field-effect Transistor," IBM J. Research/Development, Vol. 14, pp. 95-116, March 1970.
2. Reiser, Martin, "A Two-Dimensional Numerical FET Model for DC, AC, and Large-Signal Analysis," IEEE Trans. Electron Devices, Vol. ED-20, pp. 35-45, January 1973.
3. Barnes, J. T., "A Two-Dimensional Simulation of MESFETs," Ph.D. dissertation, Univ. of Mich., Ann Arbor, 1976.
4. Schroeder, J. E. and R. S. Muller, "IGFET Analysis Through Numerical Solutions of Poisson's Equation," IEEE Trans. on Electron Devices, Vol. ED-15, No. 12, pp. 954-961, December 1968.
5. Barron, M. B., "Low Level Currents in Insulated-Gate Field Effect Transistors," Solid State Electronics, Vol. 15, pp. 293-302, 1972.
6. Armstrong, G. A. and J. A. Magowan, "The Distribution of Mobile Carriers in the Pinch-Off Region of An Insulated Gate Field-Effect Transistor and Its Influence on Device Breakdown," Solid-State Electronics, Vol. 14, pp. 723-733, 1971.
7. Kennedy, D. P., "Mathematical Simulation of the Effects of Ionizing Radiation on Semiconductors," Contract No. F19628-70-C-0098, Final Report No. AF CRL-72-0257 (1972).
8. Kennedy, D. P. and P. C. Marley, "Steady State Mathematical Theory for the Insulated Gate Field Effect Transistor," IBM J. Res. Develop., Vol. 17, pp. 2-12, January 1973.
9. Mock, M. S., "A Two-Dimensional Mathematical Model of the Insulated-Gate Field-Effect Transistor," Solid-State Electronics, Vol. 16, pp. 601-609, 1973.
10. Motta, R. F., "Steady-State Theory for the Metal-Oxide-Semiconductor Field Effect Transistor," Ph.D. Dissertation, Univ. of Florida, 1976.
11. El-Mansyret, Y. A. and A. R. Boothroyd, "A Simple Two-Dimensional Model for IGFET Operation in the Saturation Region," IEEE Trans. on Electron Devices, Vol. ED-24, No. 3, pp. 254-262, March 1977.

REFERENCES (Continued)

12. Strang, G. and F. J. Fix, An Analysis of the Finite Element Method, Prentice-Hall, 1973.
13. Hohl, J. H., "Variational Principles for Semiconductor Device Modeling with Finite Elements," IBM J. Res. Develop., Vol. 22, No. 2, March 1978, p. 159.
14. Sutherland, A. D., "A Two-Dimensional Computer Model for the Steady-State Operation of MOSFETs," ARPA Report ECOM-7-1344-F Supplement, September 1977.

QUARTERLY

FINANCIAL REPORT

FOR

NASA Contract NAS8-26749

September 1, 1978 - November 30, 1978

Prepared for

George C. Marshall Space Flight Center

Marshall Space Flight Center

Alabama 35812

Submitted By

J.D. Trotter, Principal Investigator

T. E. Wade

J.D. Cassaway

COST ANALYSIS OF RESEARCH PROJECTS

CONTRACT 30-45-0210607-232 PROJECT TITLE NASA Contract NAS8-26749
 DATE THIS REPORT September 1, 1978 THROUGH September 30, 1978

	EXPENDITURES THIS MONTH	EXPENDITURES TO DATE	OUTSTANDING COMMITMENTS	FREE BALANCE	TOTAL PROPOSED BUDGET
A. PERSONNEL SERVICES					
(1) Professional					\$22,806
(2) Graduate Assistants					8,350
(3) Undergraduate assistants					1,680
(4) Technical					
(5) TOTAL PERSONNEL SERVICES	2,682.40	12,065.69		13,949.31	33,036
B. MATERIALS AND SUPPLIES	125.80	879.15		1,970.85	2,850
C. EQUIPMENT					
D. TRAVEL	874.64	998.08		1,554.92	2,553
E. EMPLOYEE BENEFITS		1,023.85		2,671.15	3,695
F. OTHER (Specify) Computer Service				3,000.00	3,000
COMMUNICATIONS		90.75		- 90.75	
G. TOTAL DIRECT EXPENDITURES					45,134
H. INDIRECT COST 45.0% of A(5)		4,915.31		9,950.69	14,866
I. TOTAL EXPENDITURES	3,689.84	26,973.83		33,026.17	\$60,000

COST ANALYSIS OF RESEARCH PROJECTS

CONTRACT 30-45-021060/-232 PROJECT TITLE NASA Contract NAS8-26749

DATE THIS REPORT October 1, 1978 THROUGH October 31, 1978

	EXPENDITURES THIS MONTH	EXPENDITURES TO DATE	OUTSTANDING COMMITMENTS	FREE BALANCE	TOTAL PROPOSED BUDGET
A. PERSONNEL SERVICES (1) Professional					\$22,606
(2) Graduate Assistants					8,550
(3) Undergraduate Assistants					1,680
(4) Technical					
(5) TOTAL PERSONNEL SERVICES	2,639.00	21,705.69		11,330.31	33,036
B. MATERIALS AND SUPPLIES	194.45	1,073.60		1,776.40	2,850
C. EQUIPMENT					
D. TRAVEL		998.08		1,554.92	2,553
E. EMPLOYEE BENEFITS	700.06	1,723.91		1,971.09	3,653
F. OTHER (Specify) Computer Service COMMUNICATIONS		90.75		3,000.00	3,000
G. TOTAL DIRECT EXPENDITURES				- 90.75	45,134
H. INDIRECT COST 45.0% of A(5)		4,915.31		9,950.69	14,866
I. TOTAL EXPENDITURES	3,533.51	30,507.34		29,492.66	\$60,000

COST ANALYSIS OF RESEARCH PROJECTS

CONTRACT 30-45-0210607-232 PROJECT TITLE NASA Contract NAS8-26749

DATE THIS REPORT November 1, 1978 THROUGH November 30 19 78

	EXPENDITURES THIS MONTH	EXPENDITURES TO DATE	OUTSTANDING COMMITMENTS	FREE BALANCE	TOTAL PROPOSED BUDGET
A. PERSONNEL SERVICES					
(1) Professional					\$22,805
(2) Graduate Assistants					8,550
(3) Undergraduate Assistants					1,680
(4) Technical					
(5) TOTAL PERSONNEL SERVICES	2,480.68	24,186.37		8,849.63	33,036
B. MATERIALS AND SUPPLIES	5.30	1,079.90		1,770.10	2,850
C. EQUIPMENT					
D. TRAVEL		998.08		1,554.92	2,553
E. EMPLOYEE BENEFITS		1,723.91		1,971.09	3,695
F. OTHER (Specify) Computer Service	213.08	213.08		2,786.92	3,000
COMMUNICATIONS		90.75		- 90.75	
G. TOTAL DIRECT EXPENDITURES					45,134
H. INDIRECT COST 45.0% of A(5)	3,047.89	7,963.20		6,902.80	14,866
I. TOTAL EXPENDITURES	5,744.95	36,255.29		23,744.71	\$60,000